Title
MEASUREMENT OF INSTABILITIES AND ION HEATING IN AN ELECTRON BEAM ION SOURCE

Authors
Levine, M.A.
Marrs, R.E.
Schmieder, R.W.

Publication Date
1984-12-01

LBL-18733
Preprint

Lawrence Berkeley Laboratory
UNIVERSITY OF CALIFORNIA

Accelerator & Fusion Research Division

Submitted to Nuclear Instruments and Methods

MEASUREMENT OF INSTABILITIES AND ION HEATING IN AN ELECTRON BEAM ION SOURCE

M.A. Levine, R.E. Marrs, and R.W. Schmieder

December 1984

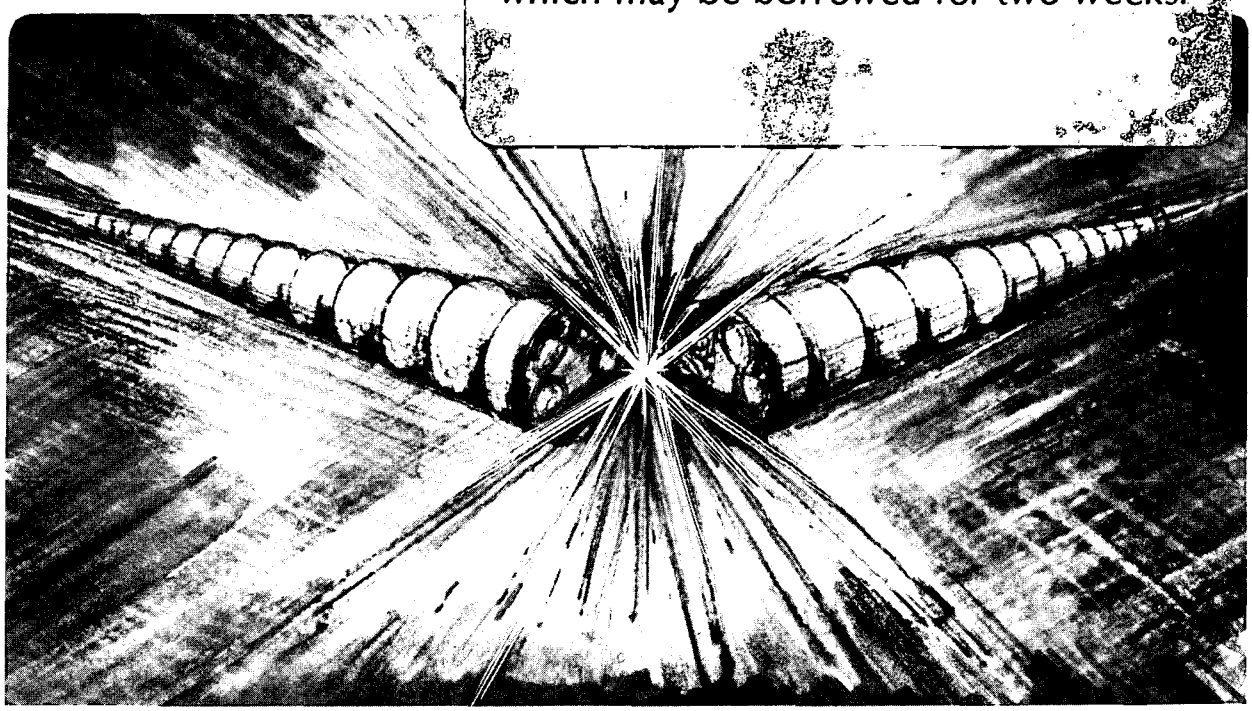

Prepared for the U.S. Department of Energy under Contract DE-AC03-76SF00098

DISCLAIMER

LBL-18733

Measurement of Instabilities and Ion Heating In an Electron Beam Ion Source*

Morton A. Levine
Lawrence Berkeley Laboratory
University of California
Berkeley, CA 94720

R. E. Marrs
Lawrence Livermore National Laboratory
Livermore, CA 94550

Robert W. Schmieder
Sandia National Laboratories
Livermore, CA 94550

December 14, 1984

Submitted to
Nuclear Instruments and Methods

* This work was supported in part by the U.S. Department of Energy under Contract Numbers DE-AC03-76SF00098 and W-7405-ENG-48.

Measurement of Instabilities and Ion Heating In an Electron Beam Ion Source*

Morton A. Levine
Lawrence Berkeley Laboratory
University of California
Berkeley, CA 94720

R. E. Marrs
Lawrence Livermore National Laboratory
Livermore, CA 94550

Robert W. Schmieder
Sandia National Laboratories
Livermore, CA 94550

Abstract

The role of instabilities in the performance of an Electron Beam Ion Source (EBIS) has been studied experimentally. Measurements were made on the EBIS test stand at the Lawrence Berkeley Laboratory using an rf spectrum analyzer, a x-ray camera and a time-of-flight analyzer. Instabilities associated with the beam current, trapped electrons and trapped ions were identified. It was found that when the instabilities were present the effective ionization rate was reduced and the radial extent of the ions was increased. These observations are consistent with the hypothesis that the ions are being heated by the instabilities.

* This work was supported in part by the U.S. Department of Energy under Contract No. DE-AC03-76SF00098.

1. Introduction

An Electron Beam Ion Source (EBIS) uses an electron beam of high current density propagated along a uniform magnetic field to trap and strip ions to high charge states. The advantage of this device over other ion sources is its potential for producing very high charge states while keeping the ion kinetic energy very small. Applications as an injector for accelerators and in the study of atomic physics[1] have stimulated renewed interest in EBIS devices, and new sources are being built in several laboratories.[2,3] In the classical model of an EBIS, ions are electrostatically trapped in the electron beam, radially by the charge of the beam electrons and longitudinally in a field created by biasing drift tubes (see Fig. 1). These trapped ions are then sequentially stripped of orbital electrons by the electron beam. Ionization stages as high as Xe^{+52} have been obtained by this method[1].

Despite the success that has been obtained using an EBIS, Donets[4] has noted anomalous behavior that might limit EBIS performance. One explanation of the anomalous behavior is the existence of plasma instabilities which heat the ions so that they escape the ionization trap.

There are several instabilities which could cause these problems such as the electron-electron two stream instability,[5] Penning electron driven instabilities,[6] current driven instabilities[7] and the ion-electron two stream rotational instability.[8] In this paper we report experimental measurements in an EBIS of rf noise, changes of the ion charge state spectrum and changes of the ion spatial distribution. The data are consistent with the existence of several instabilities and the consequent heating of the trapped ions.

2. Ionization and Trapping

An idealized model for ions trapped in an EBIS is that they oscillate radially within the electron beam and bounce back and forth between axial potential barriers at the ends of a series of drift tubes. If these ions are created from a constant source of neutrals, then there will be an evolving distribution of high charge states. As is shown in Fig. 2, the abundance of these charge states is a function of $J\tau$, the product of the current density, J and the confinement time, τ. The highest charge states result from the maximum $J\tau$.

The maximum current density, J, that can be obtained is given by the Brillouin limit. It is found by balancing the electrostatic force of the electron charge with the Lorentz force on the gyrating electron in the magnetic field, B. If a uniform beam profile is assumed, and $J = n_e e v_e$, then the maximum electron density, n_e, is given by[9]

$$n_e = 4.86 \times 10^4 B^2/(1-f), \text{ cm}^{-3} \qquad (1)$$

where B is in gauss and f is the fraction of the electron beam neutralized by ions. Theoretically a condition known as "beam collapse" might occur if f increases to 1. This would give extraordinarily high electron and current densities.

We can find the potential difference, V_b, between the center of the beam and the edge of the beam:

$$V_b = 1.51 \times 10^4 \quad \frac{I\,(1-f)}{E^{1/2}} \quad \text{Volts} \qquad (2)$$

where I is the beam current in amperes and E the beam energy in eV. Thus, QeV_b represents the maximum energy for any ion of charge, Q, created at rest

within the beam and not subject to heating. If the radial energy of the ion somehow becomes greater than QeV_b, then the ion will spend part of the time outside of the beam, and the average electron current seen by the ion will be less than the actual electron current density. Thus any mechanism which heats the ions could lead to lower average charge states (for a given confinement time, τ).

3. Ion Heating

3.1 Collisional and Potential Heating

One mechanism for heating the ions is collisions with beam electrons. However, classical calculations show that this heating is small because of the high energy of the electron beam and the averaging effect of the longitudinal oscillatory motion of the trapped ions.[10] For experiments reported here (trapping time $\approx$ 20 ms, beam energies $\approx$ 3 keV) the ions are heated to 0.1 eV. This can be compared to the beam well potential, V_b, of about 30 V.

A much larger source of ion thermal energy in the present experiments comes from the energy gained during ionization in the radial potential of the electron beam. For a uniform electron beam density, the radial potential is harmonic, $V(r) = V_b \frac{r^2}{r_b^2}$ where r_b is the beam radius. If we assume that the neutral mean free path in the electron beam is long compared to the beam diameter then the average total energy gained by a neutral ionized to $Q = +1$, is $V_b/2$. To calculate the energy gain for higher charge states we assume the beam radius is small compared to the ion gyroradius, and that the ion-ion relaxation time is short compared to the time for subsequent ionization so that the ions are thermalized. Thus, we can apply the virial theorem, which

says that the time-averaged kinetic energy in the orbital plane is equal to the time-averaged potential energy for a harmonic radial potential. Hence, 3/5 of the total energy becomes kinetic energy, equipartitioned over the two transverse and one axial degree of freedom, and 2/5 of the total energy becomes potential energy in the radial well. The maximum radius reached by a singly charged ion of average energy therefore occurs at a potential of $V(r) = \frac{2}{5} V_b$. We refer to this radius, r, as the radial extent of the ions. Repeating the same process for subsequent ionizations leads to the curve shown in Fig. 3. As can be seen, the ions should be confined to a radius significantly smaller than the electron beam; and, they stay closer to the axis as their charge increases. Any additional ion heating will tend to inhibit this confinement, spreading the ions more uniformly in the beam and beyond.

3.2 Instabilities and Ion Heating

Plasma instabilities can lead to ion heating. One illustration of how this might happen via the ion lower hybrid wave is predicted theoretically[11,12] and has been demonstrated experimentally.[13] This wave may be generated directly by an instability, but it is more probable that another higher frequency wave is generated that will stimulate the ion lower hybrid wave by parametric decomposition. The ion lower hybrid wave is then damped, transferring the wave energy into ion thermal energy. Other ion waves such as ion cyclotron waves, if stimulated, could also contribute to ion heating.

The two conditions needed to generate instabilities are present in an EBIS. First, there is a source of free energy in the directed energy of the

beam. Second, if the current is more than about 10 mA, the diameter (and of course the length) of the electron beam is larger than a Debye length. These conditions make it possible for a variety of instabilities to exist. Some of the possible instabilities are the electron-electron two stream instability,[5] Penning discharge oscillation[6] instability, the backward wave oscillator instability,[7] and the modified rotational electron-ion two stream instability.[8] We will discuss these instabilities in turn.

Both the Penning discharge and the electron-electron two stream instability depend on trapped electrons. There are several sources for these electrons including secondary electrons from the collector, electrons stripped from background gas, and electrons stripped from trapped ions. Electron trapping occurs where electrostatic potential maxima exist along a magnetic field line. In an EBIS, potential maxima normally occur at the ends of the axial trap. By raising the collector potential until no potential maximum occurs between the ion trap and the collector, it is possible to eliminate electrons held in this region. The only remaining electron trap is the potential barrier on the upstream end of the ion trap.

The backward wave oscillator instability develops when an electromagnetic wave in the beam structure is amplified by charge bunching in the electron beam. In the case of a uniform beam structure, the oscillation will exist if[7]

$$I > \frac{4E_b}{Z_o} \left[\frac{A_o}{N}\right]^3 \qquad (3)$$

where I is the beam current, E_b is the beam energy, N the length of the structure in wavelengths, Z_o the circuit impedance, and A_o a dimensionless

parameter depending on the geometry. Because of the complexity of the EBIS geometry A_o has not been evaluated. Equation 3 can be considered as an instability "turn-on" condition. The backward wave oscillator is unique, among the instabilities mentioned, in that its turn-on depends directly on the beam current.

The modified rotational electron-ion two-stream instability is a convective instability that grows in the trapped ions. Litwin, Vella and Sessler[8] (LVS) predict that the most unstable mode grows if $\gamma L/v > 1$, where L is the ion trap length, v the electron beam velocity, and

$$\gamma \simeq \frac{\sqrt{3}}{2}\left(\frac{\omega_{pe}\,\omega_{pi}^2}{2}\right)^{1/3} \tag{4}$$

Here ω_{pe} is the electron plasma frequency and ω_{pi} is the ion plasma frequency. Thus, for stability, it is required that

$$5.35 \times 10^{-5}\, L\left(\frac{n_e}{E}\right)^{1/2}\left(\frac{fQ}{A}\right)^{1/3} < 1 \tag{5}$$

where A is the atomic weight of the ion. For a typical set of conditions used in the experiments reported here, i.e., Brillouin flow, B = 3 kG, f = 0.1, Q/A = .2, E = 3000 V, it is found that $\gamma L/v > 1$ if L > 6 cm. Thus, as the EBIS trap is made longer than 6 cm more and more of the electron beam energy goes into wave energy.

4. Experimental

The Berkeley EBIS, designed and built by Brown and Feinberg, was used for these measurements. A description of this device and some results are published elsewhere.[14,15] In this device, the electron beam propagated 0.75

meter from the gun to the collector through 15 drift tubes. The drift tubes were 1 cm inside diameter and 5 cm long and were separated from each other by 1 mm. The gun had a perveance of 2 microperv. Measurements by Brown and Feinberg using a wire array gave a beam radius of 125 microns for a 250 mA beam in a 3 kG field.

In the experiments reported in this paper, the ions were created from the background gas which consisted of hydrogen, water, carbon monoxide, carbon dioxide, nitrogen and oxygen. In principle, the beam could pump out all the neutral gas in the drift tubes. (The rate of replacement of neutrals from the main chamber is small due to the low conductance of the drift tube array). A time constant, t_o, for pump-out to occur can be defined as $t_o = \pi r_o^2 n_o (dt/dN_i)$ where $n_o \pi r_o^2$ is the number of neutrals per cm in a drift tube of radius r_o and N_i is the number of ions per cm created by the beam. Thus, $t_o = \pi r_o^2 e/(\sigma I)$ where σ is the ionization cross section, I the beam current and e the electron charge. For I=0.1 A, r_o = 0.5 cm and $\sigma = 2.8 \times 10^{-17}/cm^2$ (3 keV electrons on nitrogen) we find t_o = 40 msec. This time is longer than the times of the order of 20 msec used in the experiment. Thus, the background gas provided a spatially uniform source of neutrals which were then ionized. This mode of operation (i.e., no gas injection) also allowed us to operate at the best possible vacuum, which was important in order to delay over filling the ion trap for as long as possible.

4.1 Time-of-Flight Analyzer

A time-of-flight (TOF) analyzer was used to measure the charge state distribution of the trapped ions. To accomplish this, ions were released from the trap by lowering the barrier on the collector end. The ions were then

transported through the hollow collector, past a gated deflector, and then down a 2 meter tube where they were detected with an electron multiplier. The TOF was measured from the time of the gate at the entrance of the 2 meter tube. Tests indicated that the intensity of the ion pulse was more reproducible if the electron beam was turned off just after the ion trap barrier was lowered, probably because the turn-off eliminated field variations due to asymmetries in the electron beam in the zero field region of the collector. However, this technique only measured those ions which had already been accelerated into the section between the ion trap and the collector when the electron beam was turned off. A number of pulses were averaged in which the time interval between the barrier-down time and the beam-off time was varied. This insured that the measurement was independent of the time the ions left the trap region, and was thus independent of ion mass.

4.2 RF Spectrum Analyzer

Electromagnetic radiation was detected with a Hewlett Packard model 8551B rf spectrum analyzer. The signal was obtained from the high voltage lead to drift tube #2. A 1 kΩ isolation resistor was used to decouple the high voltage driver from the drift tube. A 20 pF capacitor in series with a 48 db. amplifier was used to couple the signal into the spectrum analyzer. The system had a frequency range of 1 to 1000 MHz. Inside the vacuum tank the connection to the drift tube was made with an unshielded lead, 1 m long. This lead ran parallel to the electron beam from the collector end to drift tube #2 at a radius of about 6 cm . Thus, the coupling to the electron beam was not only through the capacity of drift tube #2, but also from the radiated field of the beam picked up by the lead.

The rf spectrum analyzer sweeps through a preselected frequency range. The shortest sweep period used was 20 ms, which is of the same order as the fill time of the ion trap. Thus, conditions were changing during a measurement. To overcome this problem, the spectrum analyzer was triggered shortly after the electron beam was started, and the intensity of any frequency as function of time could be obtained by changing the starting frequency of the spectrum analyzer. A digitizing amplifier, which could average over many machine cycles, was used to improve the signal-to-noise ratio and further improve the sensitivity of the system.

4.3 X-Ray Imaging

A gated x-ray camera was used to photograph the radial profile of the ion-electron interaction region (see Fig. 1). It consisted of a cylindrical mirror at grazing-angle and a microchannel plate (MCP) with a fiberoptic output plate. An image was obtained on polaroid film pressed directly onto the fiberoptic plate. The cylindrical mirror had a 1.9 m radius of curvature. The mirror was designed to give 50% reflectivity at 30 Å. It was gold plated, set 8 cm from the beam axis at 3.7 degrees central angle with an acceptance width of 3 degrees. The mirror cast a one-dimensional image of the beam on the MCP mounted 82 cm from the beam axis. The camera viewed through a slit in a single, double-length drift tube replacing drift tube #9 and #10.

Computer analysis, using ray tracing, predicted a 20 micron resolution width for the camera. The system was prefocused to the center of the drift tube using a laser illuminated wire, which was also used to check the resolution.

The MCP had an inconel photocathode. In order to restrict the band width of the system, a parylene film was placed in front of the MCP. This gave a band pass from 44 Å to ~ 150 Å. The MCP had curved channels with sufficient amplification so that a single detected photon could be seen as a dot (about 50 microns diameter) on the film. Most data were taken with the MCP gated on for 2 ms just before the end of the ion containment time.

With the beam on and with trapped ions, a clear beam image was recorded. With the electron beam on, but with no trapped ions, no significant signal was observed. When an image was recorded there was some scattered x-ray light from the bellows connecting the MCP to the EBIS. The scattered light was asymmetric and its intensity was proportional to the intensity of the beam image.

5. Results

It was found experimentally that there was a range of conditions under which rf noise was generated. A typical plot of the signal detected up to 1000 MHz is shown in Fig. 4. The intensity and the character of the noise were a strong function of the operating parameters. The sources of the noise were investigated in terms of the three instability regimes mentioned above, i.e., trapped electron instabilities, current instabilities, and ion instabilities.

5.1 Trapped Electron Instabilities

Trapped ions were eliminated by biasing all the drift tubes near 2 kV with just enough of a voltage gradient to expel ions. The collector voltage was varied in steps from 0 kV to 2.0 kV. The resulting spectra are shown in

Fig. 5. These spectra show a minimum in rf noise with the collector voltage set to match the drift tube voltage (i.e. the number of trapped electrons was minimized). With the collector voltage lowered to 1.5 kV and 1.0 kV the spectra show a small region of broadband oscillations at about 73 MHz. With the collector voltage lowered to 0.5 kV so that there was a 1.5 kV difference in potential between the collector voltage and the drift tube voltage, narrowband radiation at 60, 65 and 84 MHz appeared. When the collector voltage was reduced to 0 V the narrowband radiation from 3 MHz to 300 MHz grew 100-fold. A portion of this radiation is shown in the top trace of Fig. 5.

Although it is difficult to assign specific resonances to the observed rf signals, the narrow band radiation has the character of a Penning discharge[6] where narrowband wave modes such as diocotron waves, cyclotron waves, etc. are stimulated by the longitudinal oscillations of the electrons. On the other hand, the source of the less intense broadband radiation would seem to be different.

To investigate the effect of the Penning discharge on the operation of EBIS the MCP camera was used. In order to obtain a signal on the MCP camera, ions had to be trapped in drift tubes #9 and #10. This did not appreciably change the rf signal generated; so that, the Penning discharge was still present. The two images shown in Fig. 6 were taken under identical conditions except for the difference of the collector voltage. The ions were allowed to build up in the well for 12 ms, and then an image was exposed for 2 ms. In Fig. 6a the collector voltage was at 0.0 V, and in Fig. 6b the collector voltage was at 2 kV. The trace in Fig. 6a is not as dark as that of Fig. 6b indicating that the number of ion-electron collisions was reduced when the

Penning discharge was present (as indicated by the rf noise signal). Assuming that the electron beam was the same in the two cases, this result implies that the number of ions within the confines of the beam was reduced when the Penning discharge was present.

5.2 Current Generated Instabilities

Even when the collector was biased so that there was a minimum of free electrons, there were still conditions under which a rf signal could be measured on the drift tubes. Under these conditions the rf noise was a sensitive function of the electron beam current and was present even without trapped ions.

The rf signal observed for several values of the electron beam current is shown in Fig. 7. The large narrow band radiation is pickup from radio transmitters. However, if the bottom trace in Fig. 7 is compared to the top trace there is a noticeable broadband signal at about 130 and 150 MHz. This broadband signal seen on the three lower traces is absent from the upper two traces taken at lower beam current. For a given beam energy there was a threshold beam current at which rf noise could be observed.

A plot of the threshold current vs. beam energy is shown in Fig. 8 for three different values of magnetic field. The region labeled "unstable" is the region where an rf signal was observed. The linear relationship of the 3 kG instability boundary in the Fig. 8 plot of beam current vs. beam energy satisfies Eq. (3) for a backward wave oscillator "turn-on."

Although the rf signal associated with the current-generated instabilities was relatively independent of whether or not trapped ions were present, there was one exception. There was a noticeable increase in the rf

signal in the region of 170-190 MHz with ions present. Oscilloscope pictures of the rf spectrum in this region are shown in Fig. 9 for an electron current of 150 mA, well within the unstable region. In these tests the voltage on drift tube #1 was 1050 V, drift tubes #2-#4 were at 950 V, drift tubes #6-#15 were graded from 950 V to 900 V, and the collector was kept at 900 V. The voltage on drift tube #5 was set at either 1025 V to trap ions or at 950 V to expel ions. All other parameters were held constant. With drift tube #5 at 1025 V, a major component of the ions trapped was hydrogren. The calculated value of the hydrogen lower-hybrid frequency is 196 MHz. The observed rf signal from 170-190 MHz is close enough to 196 MHz (within experimental error) to suggest that it is due to ion lower hybrid waves being stimulated.

The TOF analyzer was used to measure the effect of the current instability on the ions. This was done by examining the ions from a short ion trap, 15 cm long, created by selective biasing of the drift tubes. The trap was created in two positions, first near the electron gun end and then near the collector end. Data such as those shown in Fig. 10 were obtained. From these data the abundance ratio of N^{5+}/N^{4+} was compared to the computed ion abundance vs. $J\tau$ shown in Fig. 2. Thus, from a measured N^{5+}/N^{4+} ratio and the ion trapping time, τ, an effective current density was obtained.

In Table 1, the effective current density at the gun end and the collector end are given for three sets of conditions. The actual current density in EBIS was measured previously[15] using a wire array. In the wire array measurements it was found that the variation in current density from end to end in the region of uniform magnetic field was small.[16] Thus, the sharp decrease in the effective current density shown for the trap at the

collector end relative to the gun end, for large rf noise conditions, suggests that the ions are heated more at the collector end and therefore spend less time in the electron beam. This implies that the waves which heat the ions grow along the electron beam.

5.3 Ion Instabilities

Tests using the MCP camera indicated that instabilities may be present even when the rf signal was not detected. A series of tests was run with the electron beam parameters well into the stable region shown in Fig. 8, and the collector bias set to minimize the number of trapped electrons. Under these conditions rf noise could not be detected by the spectrum analyzer. An ion trap was established with a 60 mA beam current and a 60 V barrier. The calculated potential at the edge of the electron beam is 28 V. Thus, ions confined in the well were not necessarily confined in the beam. A series of MCP camera pictures was taken using ion traps of different lengths, and the x-ray intensities/cm of trap length are plotted in Fig. 11. The intensity/cm of the x rays when the trap was 40 cm long was less than the intensity/cm of the x rays when the trap was 10 cm long. It follows that the ion-electron interaction was reduced when the ion trap was long.

It was necessary to measure the number of ions per unit length in the trap to determine if the reduced ion-electron interaction was due to a loss of ions or, as hypothesized, ions being heated so that they spend part of their time outside the beam. To do this, the TOF analyzer was not gated; so that, the pulse was integrated over all of the charge states. Under these conditions, the pulse height is proportional to the number of ions/unit length. The results for traps of different length are shown in Fig. 11.

In Fig. 11 the decrease in ions/cm as the trap length is increased from 10 to 40 cm is 20%. The decrease in x-ray intensity/cm as the trap length is increased from 10 to 40 cm is 49%. Since the x-ray intensity is proportional to the number of ion-electron collisions, this result implies a decrease in the number of ion-electron collisions per ion. This decrease in the number of collisions per ion can be explained by the conjecture that the ions have been heated to a temperature higher than QeV; so that, the ions are only partially confined to the electron beam. This increase in heating with trap length connotes an instability that grows in the ions.

As another check of this hypothesis the effective current density was also measured from the N^{5+}/N^{4+} ratio as above. For a 15 cm well with 70 mA the effective current density from the N^{5+}/N^{4+} ratio was 65 A/cm^2. When the well length was increased to 40 cm, the N^{5+}/N^{4+} ratio gave an effective current density of only 29 A/cm^2. This confirmed the hypothesis that the ion-electron collision rate was reduced in a long trap as inferred from the MCP x-ray camera results noted above.

In order to test the classical theory for the ion temperature which neglects instability heating, an attempt was made to create the "most stable" conditions possible. The collector was biased to sweep out electrons. A short ion trap (10 cm) was used. Beam current and voltage were set away from the "unstable" boundary. A series of tests was run using the MCP x-ray camera with a 2 ms gate to examine the ion density as a function of time. A densitometer was then used to obtain radial intensity profiles as shown in Fig. 12 for four different times. At 5 ms the intensity of the signal was

low. However, the profile is clearly discernible with a diameter of roughly 100 μm. At 10 ms the intensity has increased, and the profile has a slightly larger diameter. The profiles at both 15 ms and 20 ms are 300 μm wide, which represents the diameter of the electron beam measured previously.[15] These results imply that the ions represented in the 5 ms profile are confined to the center of the beam as predicted by classical theory (see Fig. 3). As shown in Eq. (5) the LVS instability is weakly sensitive to the ion density. The expansion of the observed channel to 300 microns in the 15 ms and 20 ms traces, as the trap fills with ions created from the background gas, could be due to instability heating that develops at higher ion densities or it could be due to beam neutralization which lowers the electrostatic potential confining the ions. On the other hand, the existence of a narrow peak indicates that instabilities, if present, give negligible ion heating. It should also be noted that the Eq. (5) stability condition is satisfied using electron densities calculated from Table 1 and f = .25.

6. Discussion

In order to obtain the highest quality electron beam in the Berkeley EBIS, great care was used in the design and installation of the magnetic field and the electron gun. The thought was that if Brillouin flow could be attained, "beam collapse" might be achieved (see Eq. (1)). Brown and Feinberg suggest that some of their data indicates larger values of the effective J than the measured J. However the increased J was far less than might be expected. The current set of measurements would indicate that plasma instabilities which heat the ions may be the reason that "beam collapse" is difficult to attain.

The instabilities that were measured existed in three regimes. They involved free electrons, beam current and trapped ions. The LVS instability may be the most limiting because it was always unstable except when the ion trap was very short. Complete stability, as indicated in Fig. 12, was only observed with a short trap and reduced ion density. However, there is a need to confirm the findings of this report by conducting experiments in a cryogenic machine in which the ion density can be controlled over a longer experimental time than was possible in the Berkeley EBIS.

Acknowledgments

The authors wish to thank Dr. Benedict Feinberg for his advice in using the Berkeley EBIS and permission to use his computer codes and acknowledge the invaluable contributions of James Galvin to the technical design and maintenance of the equipment and Phillip Smith for help in making the rf measurement and taking data. The authors also wish to express their appreciation for technical discussions with Drs. Wulf B. Kunkel, Richard E. Fortner and John Vitko.

This work was supported by the U.S. Department of Energy under contract # DE-AC03-76SF00098.

References

(1). E. D. Donets, Physica Scripta T3, (1982) 11.

(2). J. Arianer, C. Goldstein, H. Laurent, M. Malard, IEEE Trans. Nucl. Sci. NS-30 (1983) 2737.

(3). V. O. Kostroun, E. Ghanbari, E. N. Beebe, S. W. Janson, Physica Scripta T3, (1982) 47.

(4). E. D. Donets, Fiz Elementar Cha. i atom. Ya. 13 (1982) Edition 5.

(5). R. C. Davidson, "Methods in nonlinear Plasma Theory" Academic Press, NY (1972).

(6). V. V. Vlasov, V. I. Panchenko, A. M. Rozhkov, K. N. Stepanov, V. I. Fannik, Sov. Phys. Tech. Phys. 20 (1976) 622.

(7). L. R. Walker, J. of Appl. Phys. 24 (1953) 854.

(8). C. Litwin, M. C. Vella, A. Sessler, Nucl. Inst. and Meth., 198 (1982) 189.

(9). M. C. Vella, Nucl. Inst. and Meth. 187 (1981) 313.

(10). R. Becker 2nd EBIS Workshop Saclay, ORSAY, Editor J. Arianer, E. T. Olvier (1981) 185.

(11). M. Porklab, Nucl. Fus. 12 (1972) 329.

(12). A. B. Kitsenko, V. I. Panchenko, K. N. Stepanov, V. F. Tarasenko, Nucl. Fus. 13 (1973) 557.

(13). V. F. Tarasenko, A. B. Kitsenko, V. I. Panchenko, K. N. Stepanov, Sov. Phys. Tech. Phys. 17 (1973) 1599.

(14). B. Feinberg, I. G. Brown, K. Halbach, W. B. Kunkel, Nucl. Inst. and Meth. 203 (1982) 81.

(15). I. G. Brown, B. Feinberg, Nucl. Inst. and Meth. 220 (1984) 251.

(16). B. Feinberg, Private Communication.

Table 1: Effective current density as obtained from the TOF analyzer.

Beam Current mA	RF noise	effective current density A/cm^2	
		Gun	collector
70	none	65	66
100	small	70	65
120	large	96	55

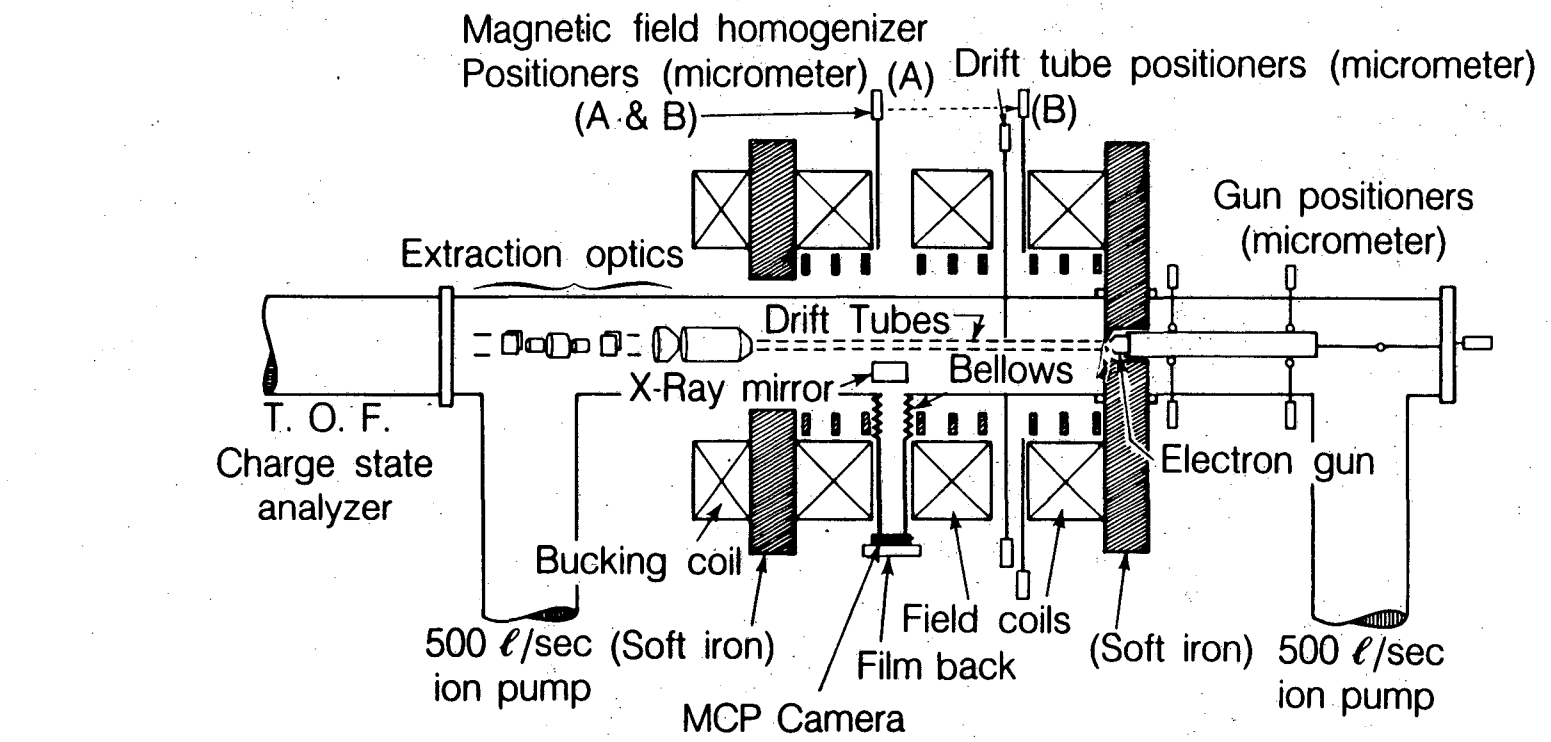

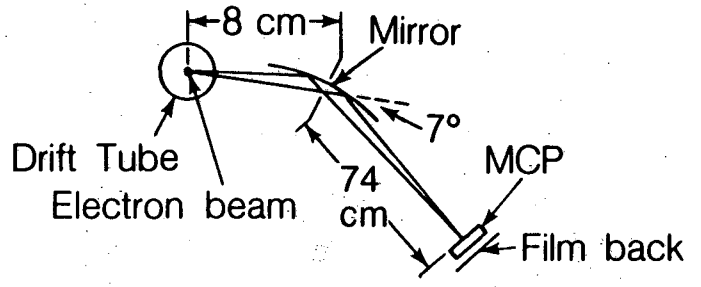

Detail inset of MCP x-ray camera

XBL 849-10866

Fig. 1 Berkeley EBIS schematic showing microchannel plate x-ray camera and TOF analyzer.

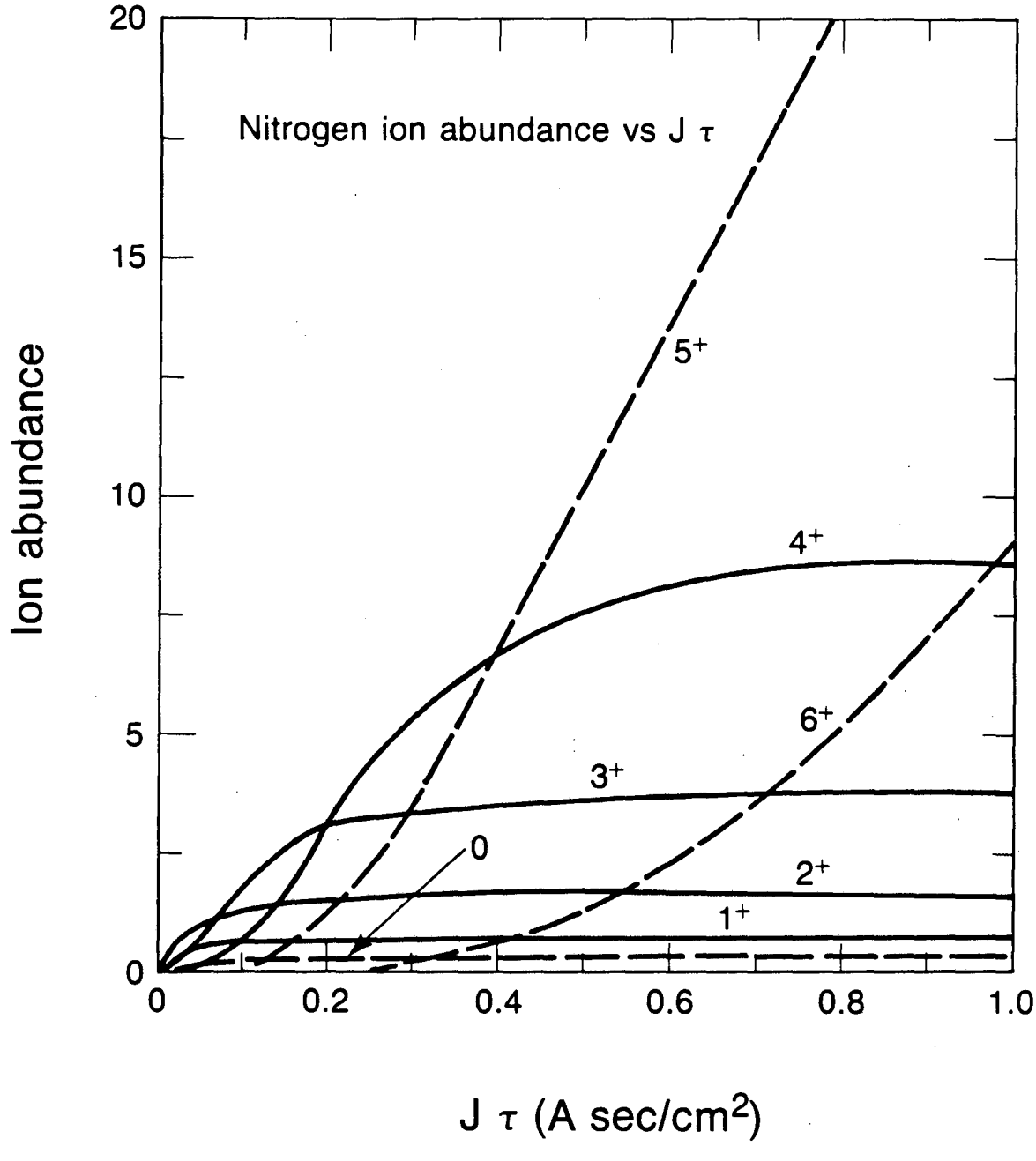

XBL 849-10823

Fig. 2 Calculated nitrogen charge state abundance for a 2250 V electron beam with ions continuously created from background gas.

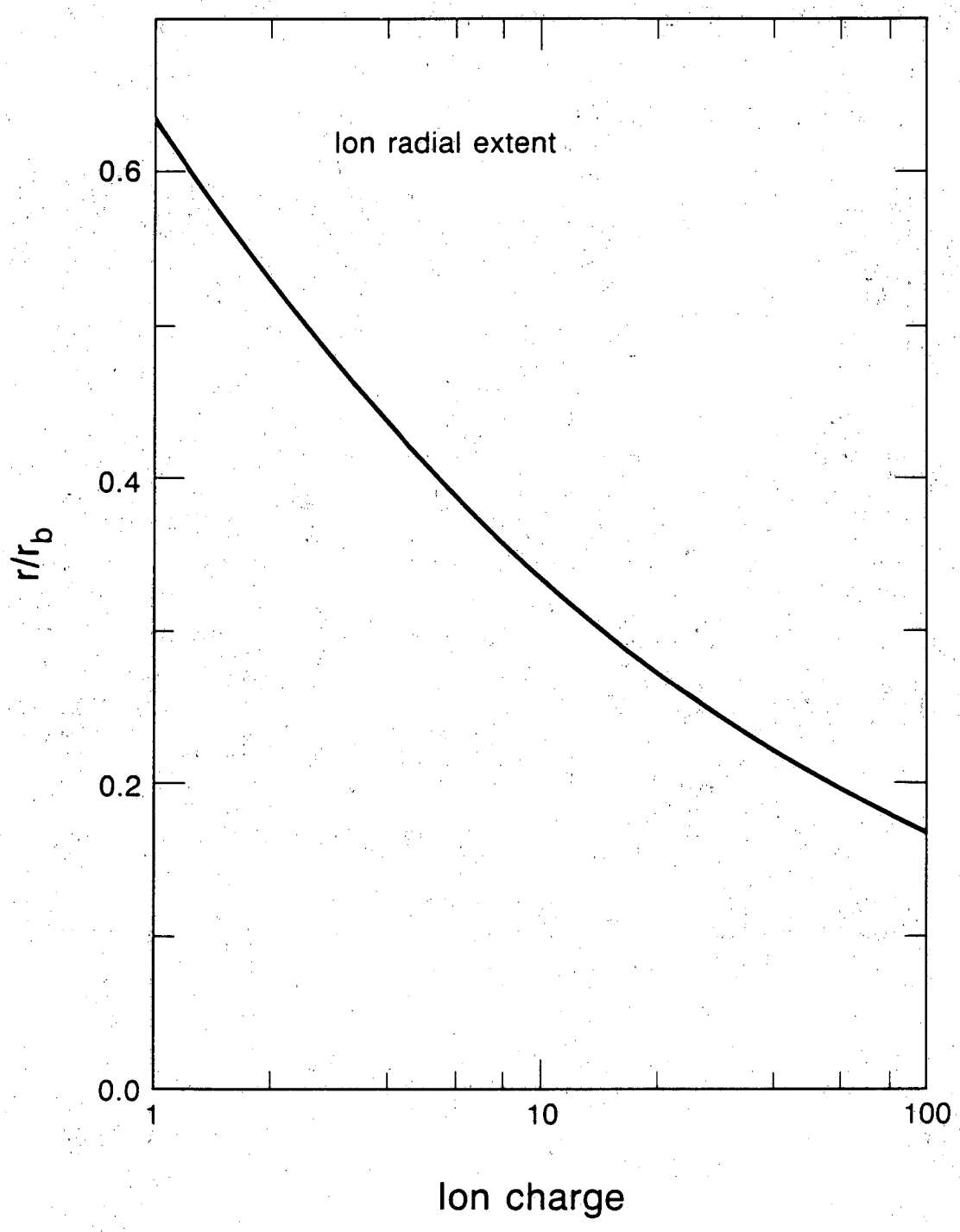

XBL 8411-6301

Fig. 3 Radial extent for an average ion vs charge state assuming: 1) ion thermal equilibrium, 2) ionization from cold background gas, 3) energy is derived from beam radial potential (space charge), 4) uniform electron density in the beam and negligible ion space charge.

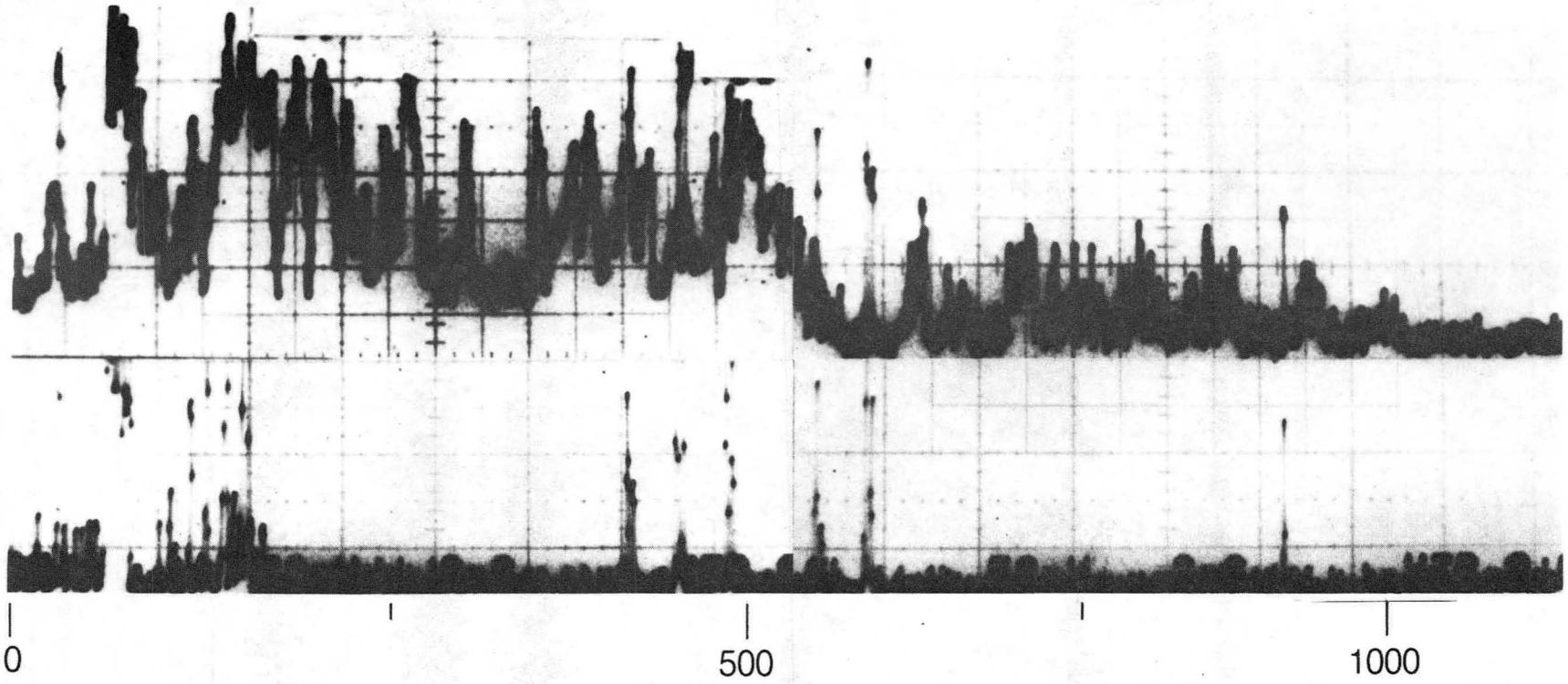

XBB 848-6310B

Fig. 4 Composite spectrum analyzer trace showing the rf signal associated with the beam. Top: electron beam on; bottom: electron beam off.

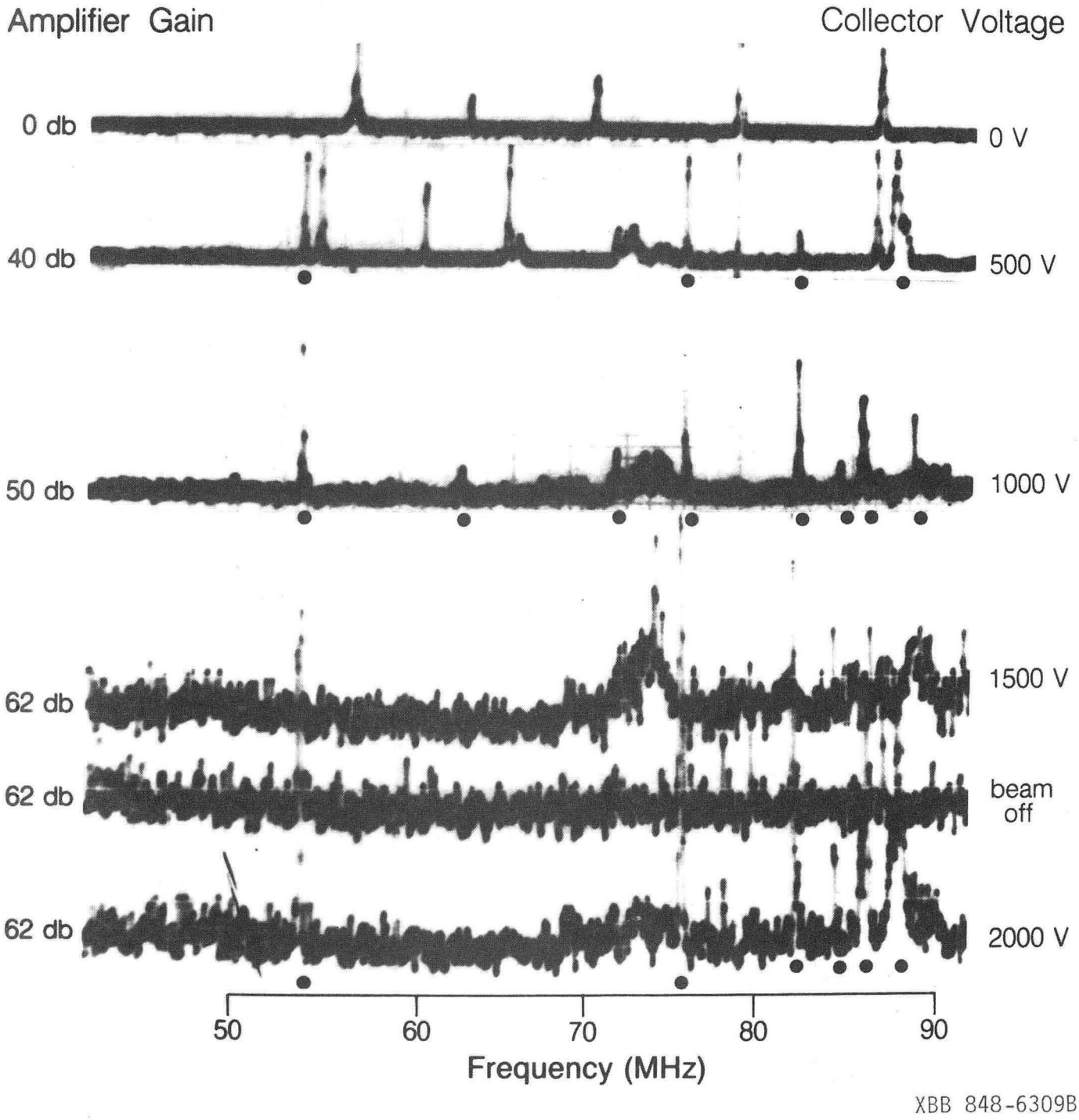

Fig. 5 RF spectra for several values of the collector voltage (V) and amplifier gain (db). The dots mark pickup from radio transmitters.

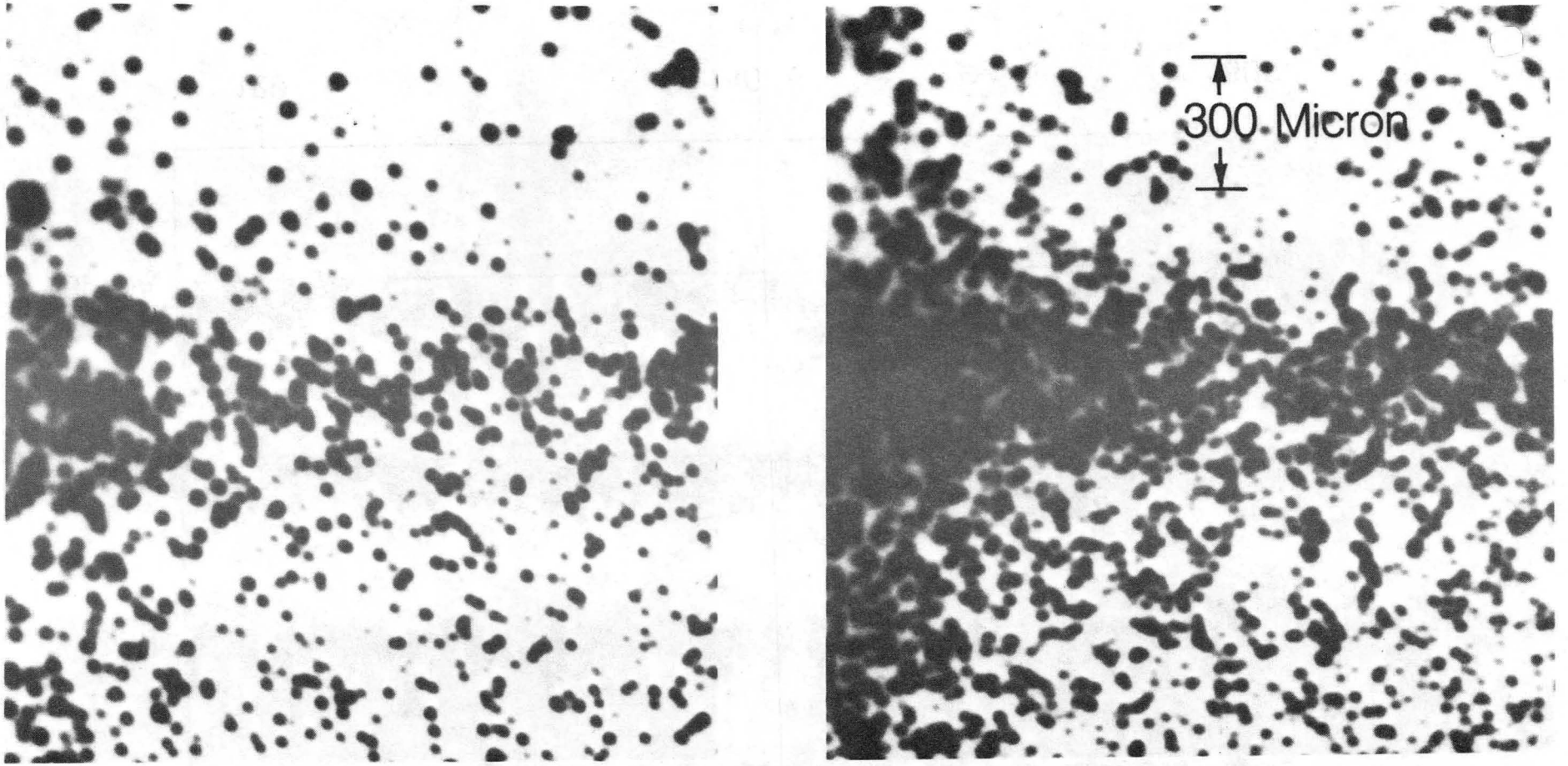

XBB 848-6312

Fig. 6 X-ray camera images of the electron beam. Shading to the left in each image is scattered light.
a. Collector voltage (0V) much less than trap voltage.
b. Collector voltage (2000V) equals trap voltage.

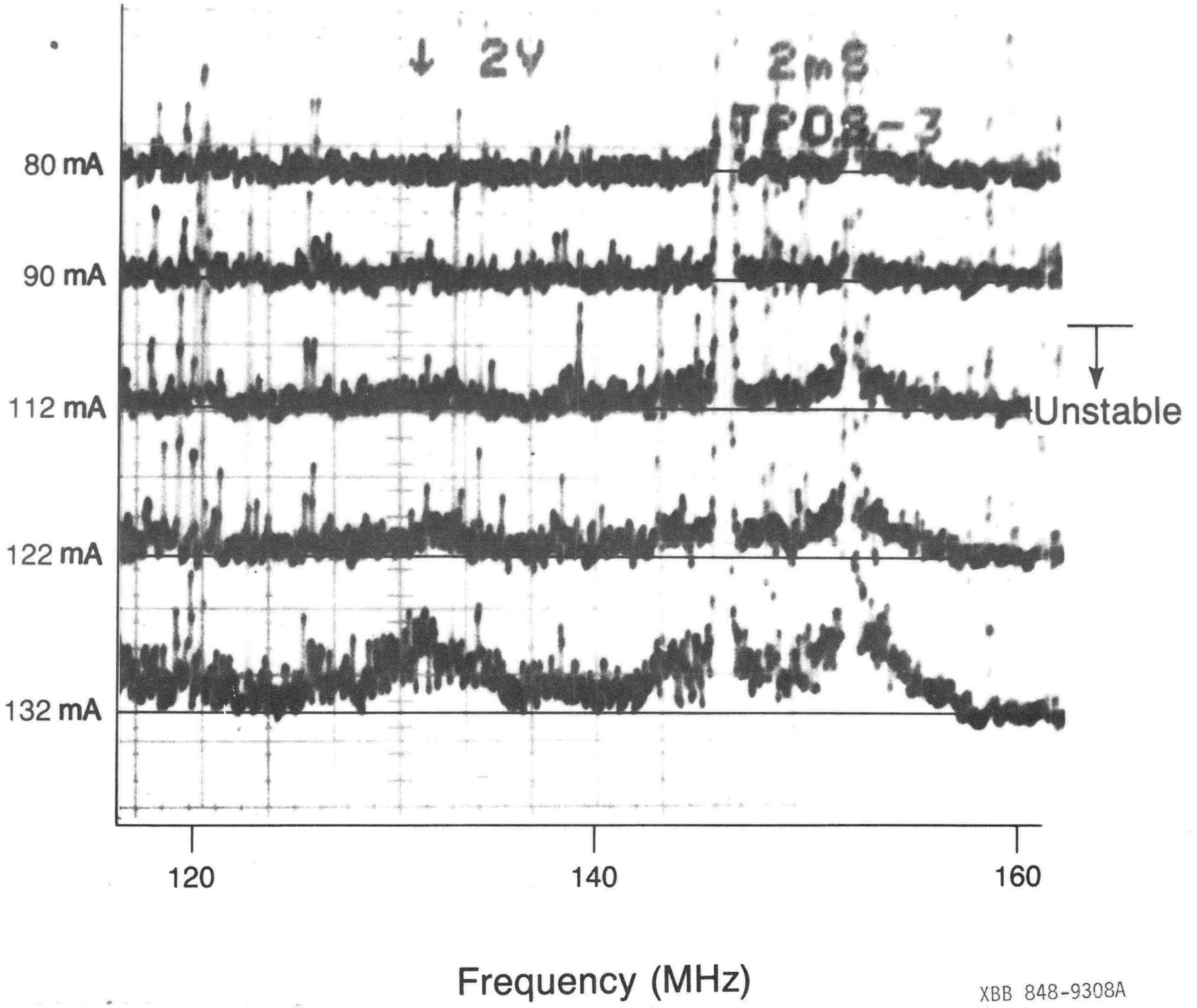

Fig. 7 RF spectra for several values of beam current. The large narrowband signal is pickup from local broadcast stations. The broadband noise near 132 and 152 MHz on the lower three traces is from the EBIS.

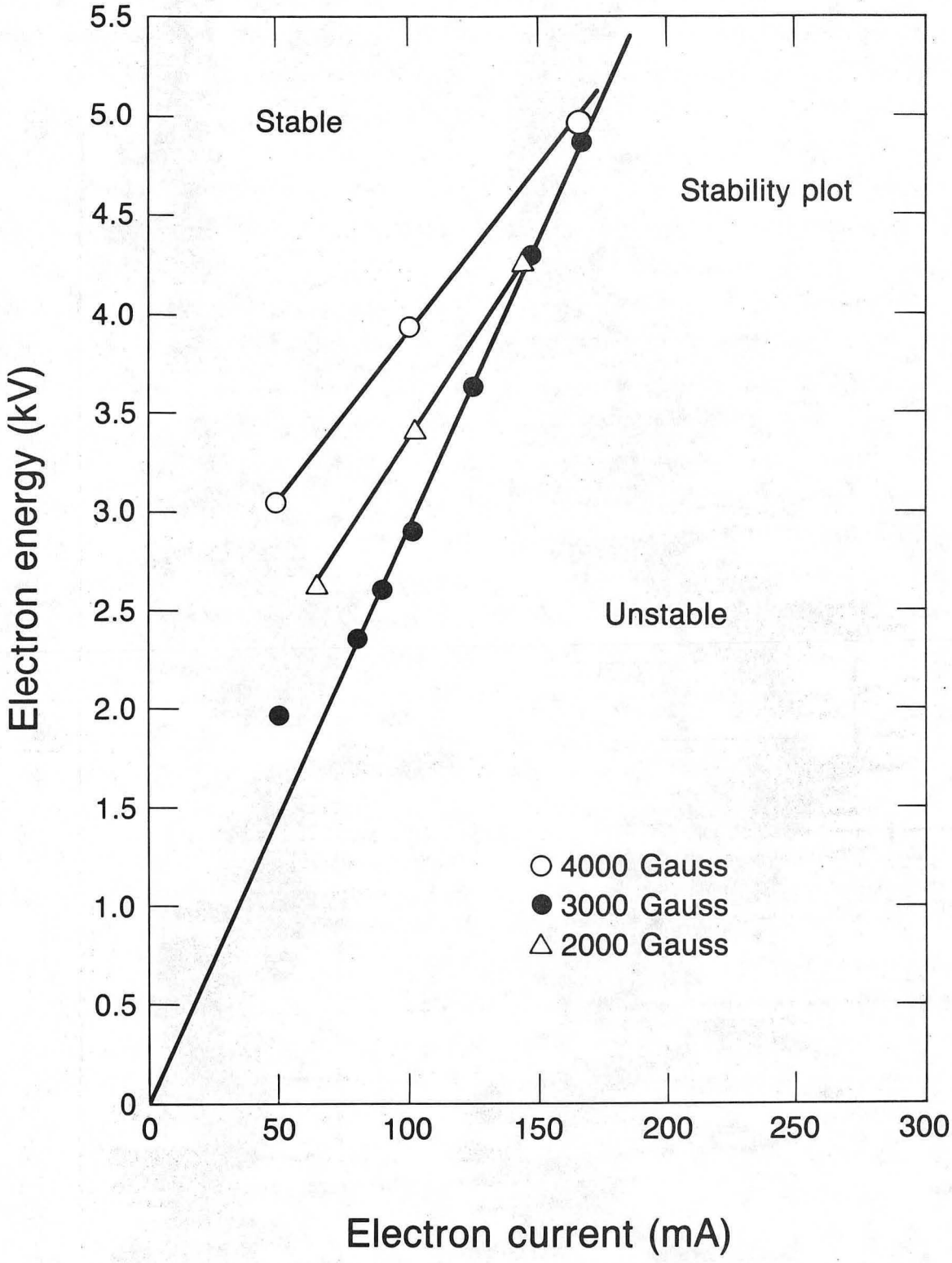

XBL 849-10826

Fig. 8 Stability boundary in the electron beam energy-current plane for three values of magnetic field. Plot is inferred from sets of rf traces such as Fig. 7.

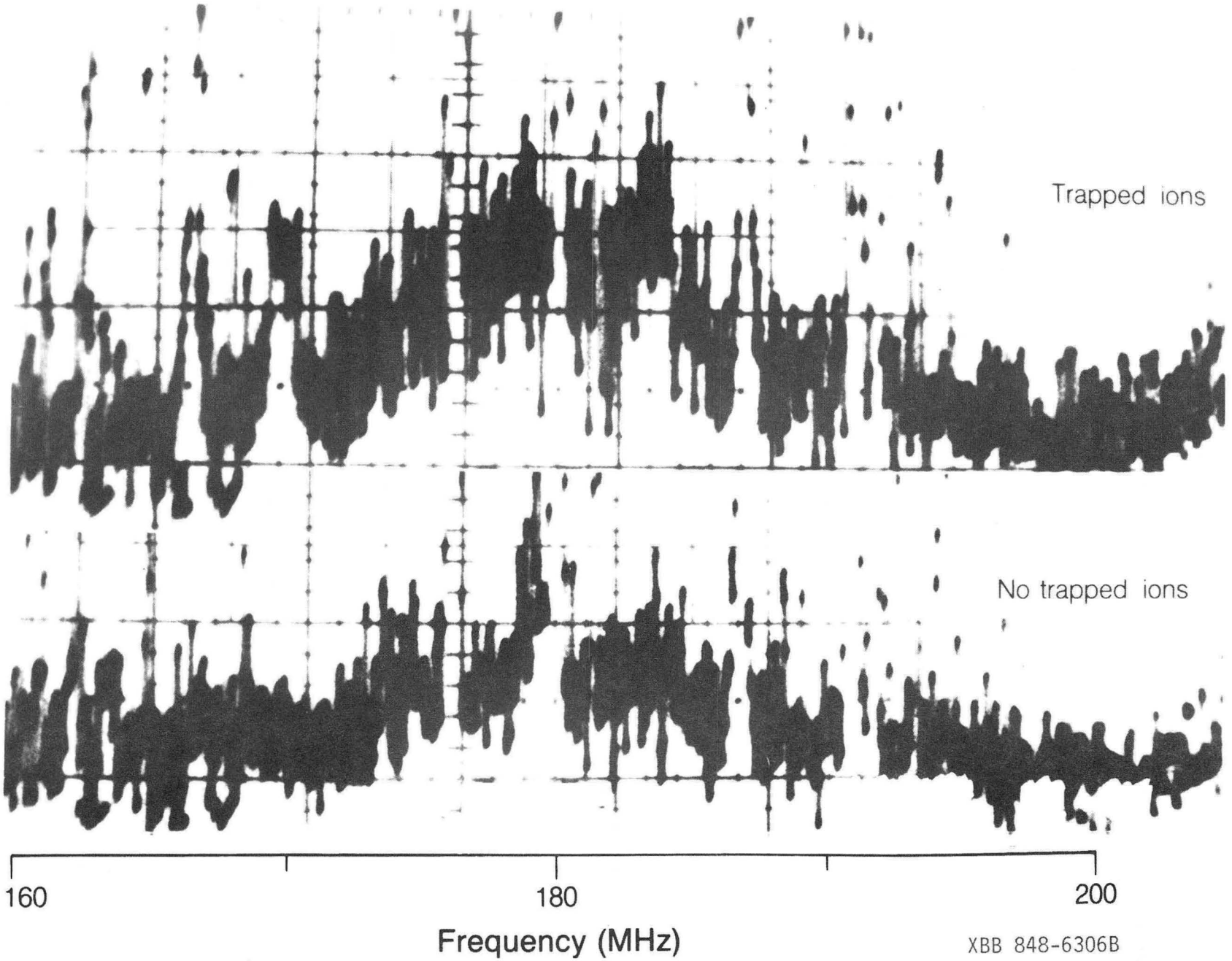

Fig. 9 RF spectra, with and without trapped ions. Upper trace is with trapped ions and shows an increase in broadband noise in the region of 170 MHz to 190 MHz.

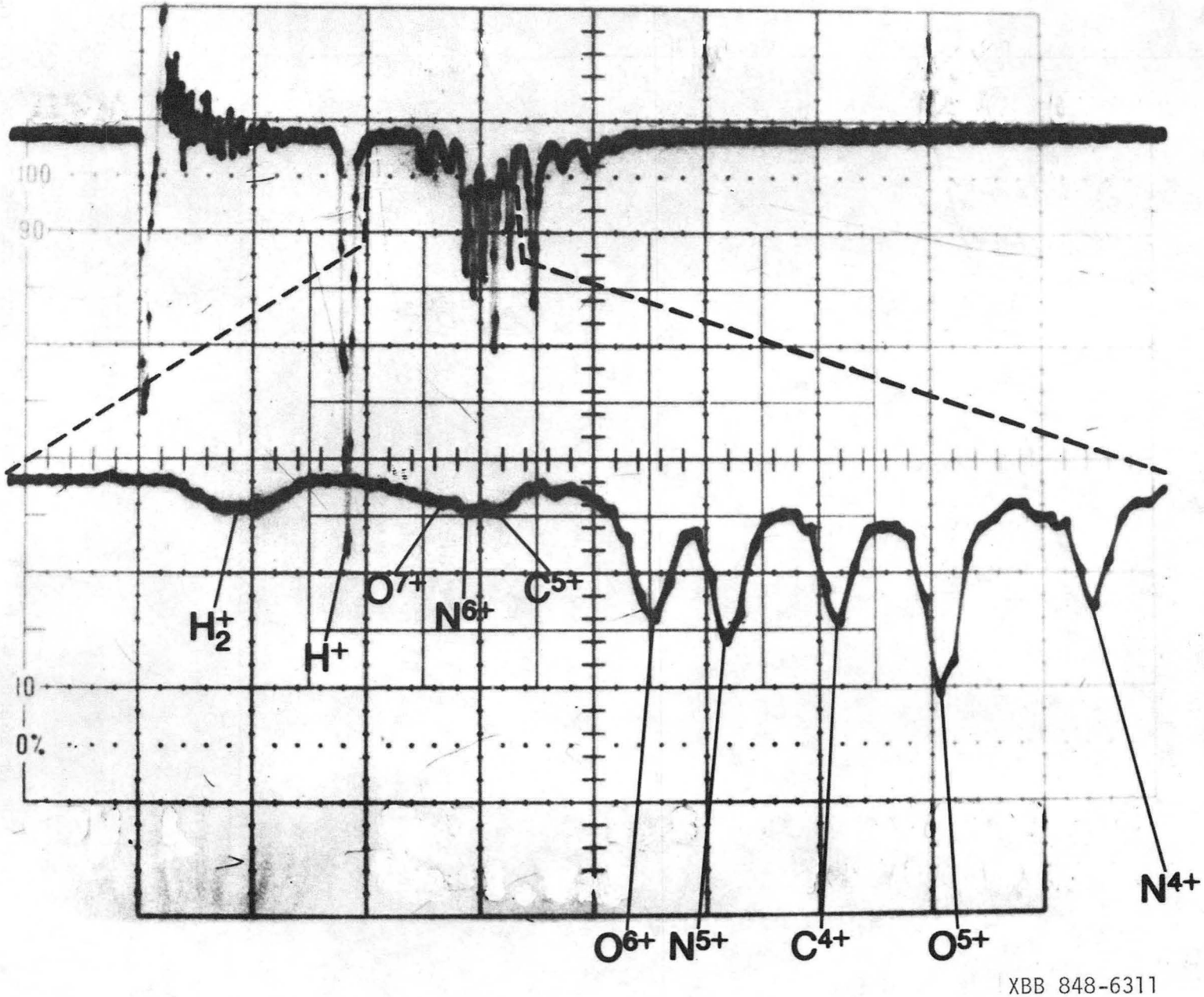

XBB 848-6311

Fig. 10 Time-of-flight analyzer spectrum for a trap at the collector end and a beam current of 120 mA. Lower trace is an expansion of the upper trace.

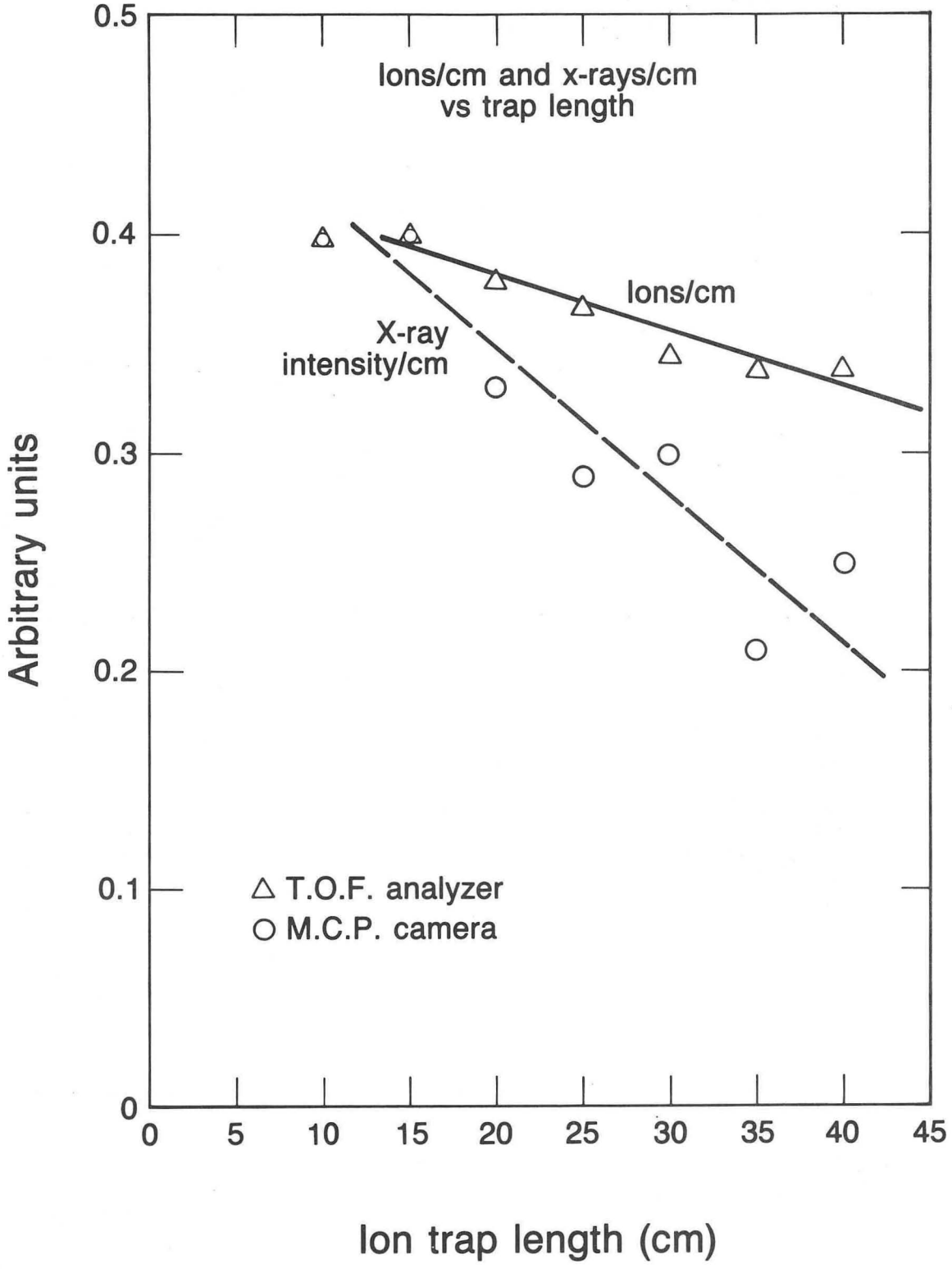

XBL 849-10824

Fig. 11 Ions/cm (measured with TOF analyzer) and x rays/cm (from x-ray camera images). Points have been normalized to the same maximum. Straight lines are drawn to guide the eye.

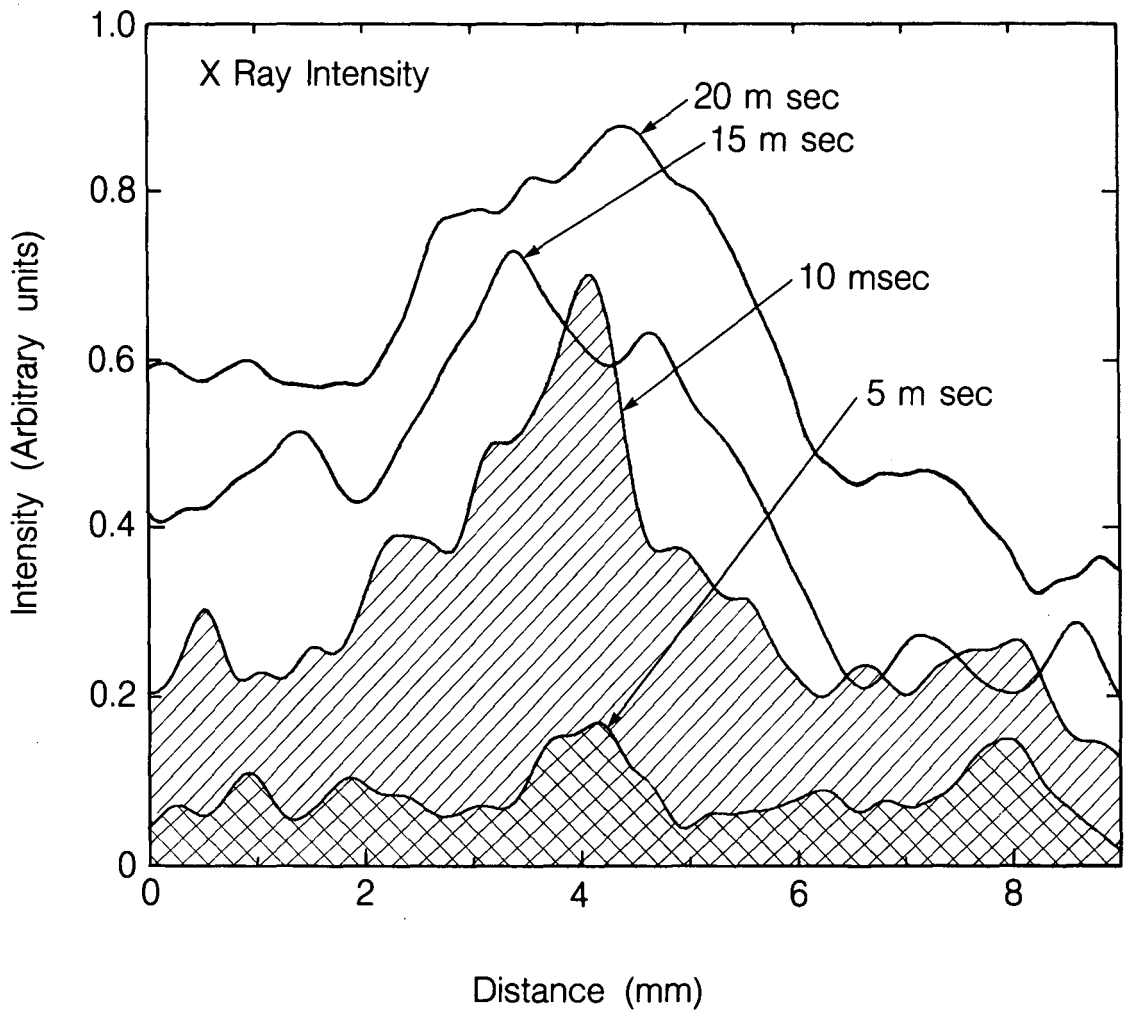

XBL 849-10865

Fig. 12 Densitometer traces of x-ray camera images at several different times. Horizontal scale refers to the image, and can be converted to electron beam coordinates by dividing by 9.3.

This report was done with support from the Department of Energy. Any conclusions or opinions expressed in this report represent solely those of the author(s) and not necessarily those of The Regents of the University of California, the Lawrence Berkeley Laboratory or the Department of Energy.

Reference to a company or product name does not imply approval or recommendation of the product by the University of California or the U.S. Department of Energy to the exclusion of others that may be suitable.

TECHNICAL INFORMATION DEPARTMENT
LAWRENCE BERKELEY LABORATORY
UNIVERSITY OF CALIFORNIA
BERKELEY, CALIFORNIA 94720